International Journal of Science and Research (IJSR)
ISSN: 2319-7064
SJIF (2022): 7.942

Synthesis and Characterization of Copper (Cu) - Doped Tungsten Oxide (WO3), Photocatalyst for Degradation of Rhodamine B Dye

G. Thirumoorth[1], B. Gnanavel[2]

[1]PG& Research Department of Physics, Government Arts College, (Autonomous) Salem 638 007,Tamilnadu India
Mail ID - thiruphysics1994[at]gmail.com

[2]PG & Research Department of Physics, Chikkaiah Naicker College, Erode, 638 004Tamilnadu, India

[3]PG&ResearchDepartmentofPhysics, Government Arts College, (Autonomous) Salem638007Tamilnadu, India

Abstract: ***The influence of copper (Cu) in determining Photocatalyticbehaviour of WO3 prepared by microwave irradiation technique (2.45GHZ, 180 W/10 min). It deals the synthesized oxygen deficient nano spherical like morphology by adopting a novel microwave irradiation technique action method with and without dopant (Cu). The powder XRD results confirmed the as prepared samples in both the cases to be orthorhombic phase (WO3·H2O) and the annealed samples (W17O47) were indexed as monoclinic structures. Microscopic observation clearly demonstrated the dopant in shaping surface morphology through formation of sheet like structure with the desired dimensions in length and width which served as building blocks for the formation of WO3 nanoparticles. The UV–Visible analysis indicated the band gap energies of the doped samples to be lighter than that of surfactant free samples. These observations suggest that the doped nanomaterials may be suitable for photo catalytic applications and the oxygen vacancy may be used to induce the changes in electrical properties.***

Keywords: Tungsten oxide, Microwave irradiation, Copper doping, VSM

1. Introduction

The nanosized materials have attracted great attention as a result of exhibiting a unique surface - to - volume ratio. In particular, high surface area materials have been of great interest in a wide range of applications such as catalysis, chemical and biosensors, fuel cell electrodes, and so forth [1]. As a well - known inorganic oxide, WO3 is a promising candidate for many applications such as electrochromic [2], photocatalytic [3], photoluminescent [4], and as a gas sensor device [5] due to the existence of various structural polymorphs and easily tunable oxygen content of the end product by varying the growth atmosphere. The optical and electrical properties of this compound strongly depend on the size and morphology of the corresponding end product. Accordingly, the recent scenarios for many practical applications are mainly based on the morphology and size distribution of the nanoparticles. This can be done by varying the synthesis procedure and growth atmosphere which influence the morphology and size distribution of the nanoparticles. On the other hand, dopants have offered relatively better morphology and a high surface - to - volume ratio of nanoscale materials. To date, the following methods have been adopted to synthesize pure and doped WO3 in the form of powders; vapor deposition [6], hydrothermal route [7], sol - gel [8], acidification method [9], electro spinning method [10], electro deposition method [11], etc. However, the abovementioned techniques are more time - consuming and cost - effective.63 Great efforts are being taken to explore new synthesis methods to control the morphology and size distributions to satisfy certain applications. Recently, most of the works focused on the preparation of doped nanocrystalline WO3 following their successful applications. Zhu et al. have prepared Cu - doped WO3 materials with photonic structures using a combined sol - gel templating and calcinations method for the detection of various volatile organic gases. They suggested that the photonic crystal of the Cu - doped WO3 replica sensor has a much higher response as well as selectivity when compared to that of the pure one due to their different morphologies [12]. Change fabricated Zn - doped WO3 thin films and found the enhanced behavior of Zn - doped WO3 with a suitable amount in the case of photocurrent and photo - activity [13]. Zamani et al. have synthesized Cr - doped mesoporous WO3 nanomaterial by chemical route for the detection of amines and tetramethyl amines. Finally, they summarized the product showed low sensitivity to NH3, and TMA was detected more efficiently [14]. Xia et al. have prepared pure and Au - doped WO3 nano powders by a colloidal chemical method. They concluded that proper Au loading on WO3 is suitable for the detection of NO2 at relatively low temperatures [15]. Kalidindi et al. fabricated Ti - doped WO3 films on Si (100) wafers using the sputtering technique and found that the electrical conductivity of Ti - doped samples at room temperature is more than that of the pure sample [16]. With this basis, bear in mind the role of dopants in nanocrystalline WO3. H2O and WO3, we have been able to synthesize cobalt - doped WO3. H2O nano powders with different W/Co (0.02 and 0.05) ratios using simple, efficient straight forward microwave irradiation method. The procedure reported here, to the best of our knowledge, is the first demonstration in the synthesis of cobalt - doped WO3. H2O nanopowders. In the microwave irradiation method, the time required for the synthesis was around 10 min only and the reaction process was also very simple.

2. Experimental Details

Pure and doped hydrated tungsten oxide (WO3. H2O) nanoparticles were prepared by microwave irradiation method at room temperature and without employing the hydrothermal method during the synthesis process [17]. An analytical grade of 4.98g (around one molar ratio) of tungstic acid (H2WO4) was dissolved in 20 mL of sodium hydroxide (NaOH). The obtained solution was yellow and it was stirred for 20 min under ambient conditions. This may be due to the proton exchange protocol process [18]. Subsequently, 2 wt. % and 5 wt. % of copper sulphate were mixed along with tungstic acid which was added to 20 mL of deionized water. The final solution was slowly mixed and stirred again for 20 min. The pH of the solution was found to be neutral (7.0) due to the salty nature of the mixed solution and it was adjusted to 1 with the addition of HCL because it can act as a precipitating agent and also a medium for the product to have desired morphology [19]. In addition to the above solution, 5 ml double distilled water (i. e., 50 vol. % of precursor solution) was added to the above solution to respond to microwaves quickly. The final solution of both pure and doped samples was transferred into a microwave oven (2.45GHz and maximum power of 900 W) in ambient conditions and kept at 600 W for 10 min. The resultant yellow precipitate was annealed in a tubular furnace at 600^{o} C for 6 h in the air to remove the subproductsand to improve the crystallinity.

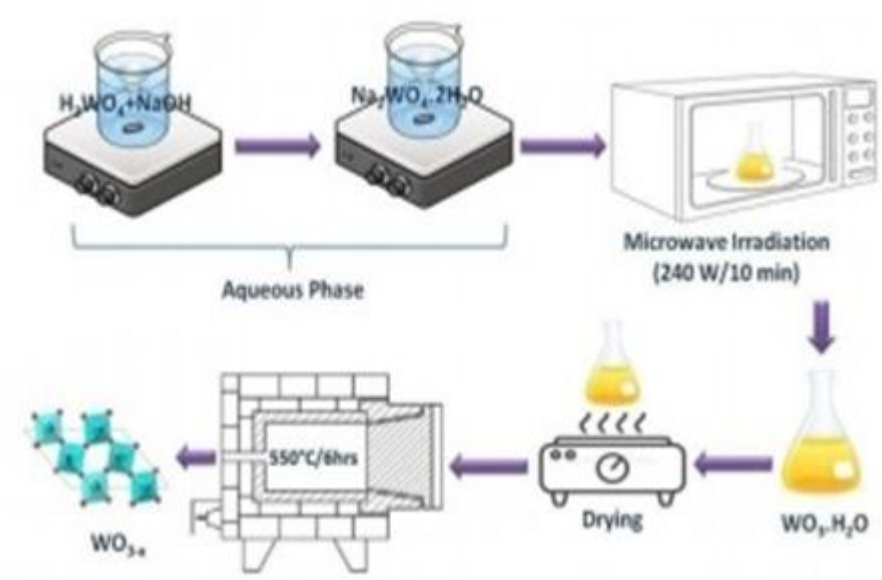

3. Results and Discussion

3.1Powder XRD analysis

Fig.3.1 a) reveals the obtained powder XRD pattern for doped hydrated tungsten oxide and Fig.3.1 b) Shows the pattern for respective annealed samples. The powder XRD patterns of pure WO3. H2O and annealed WO3 - δ have been analyzed in the previous works in detail as mentioned as a reference. The Powder XRD results confirmed the orthorhombic phase formation of WO3. H2O with improved crystalline nature in agreement with JCPDS reference no: 43 - 0679. Also, it is to be noted that a small shift in the smaller Bragg angle side for the doped (0.02) sample indicates the incorporation of dopant ion in WO3. H2O crystalline lattice due to significant atomic radii of dopant ion. On the other hand, the re attainment of crystallite site for manganese (5 Wt. %) was near to the Bragg‟s value of pure sample along (020) plane resembled the incorporation of Cu ion in WO 2 - (020) tetrahedron structure, not in water molecule site (111) which is another confirmation for the attainment of original parent phasenature.

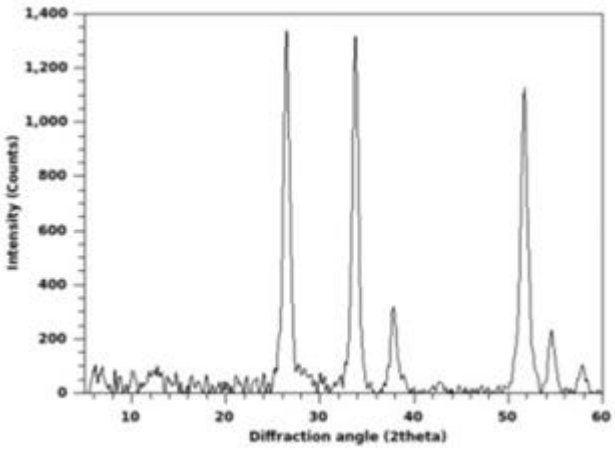

Figure 3.1: a) Representative powder XRD pattern of doped WO_3. H_2O

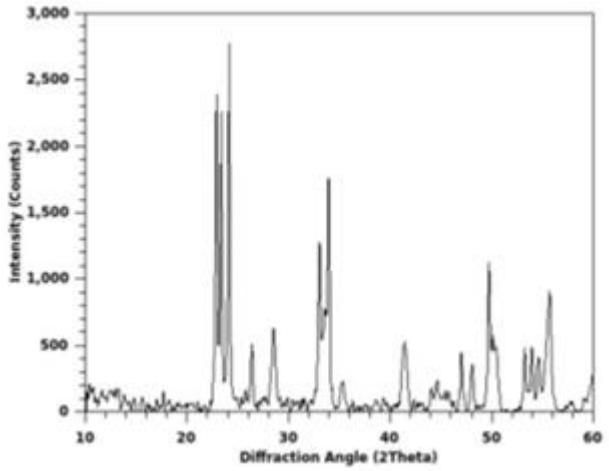

Figure: 3.1 b) Representative powder XRD pattern of annealed (doped) WO_3

3.2 Microscope analysis (FE - SEM)

The microscope analysis was carried out for the resultant as prepared and annealed nanoparticles of pure and doped tungsten oxides on an aluminum substrate are shown in Fig.3.2 a) This FE – SEM resembles the formation of sphere - like morphology agglomeration having in the order of 1 – 2.5 µm on the longer axis and 1 - 2 µm on the shorter axis. Also as additional information, the close examination revealed that plates lying parallel to the surface of the substrate and normal to the surface are rare that indicating the growth of the b axis corresponding to the (020) plane which is in agreement with the Powder XRD analysis. Above all this phenomenon arising in edge, effects were also arisen due to charge transfer between „W" and „O" ions present in the plates that have been marked in Fig.3.2 a). Fig.3.2 b) shows the annealed pure and doped WO3 - nanoparticles. It is also having an agglomerate in nature with polydisperse nature with a sphere - like morphology of the order of 4 – 5 µm on the lateral axis and 2 - 3 µm on the longitudinal axis. This may be because of the agglomeration of fast and rapid collision between the particles during the recrystallization process because of the annealing effect. The attainment of a highly uniform with high crystalline nature than the pure sample illustrated the role of dopants in modifying the morphology of the end products especially annealed samples. Also, oxygen content plays an important role in fixing the condition for morphology, because the percentage of oxygen in the copper doped sample is more than that of the pure sample

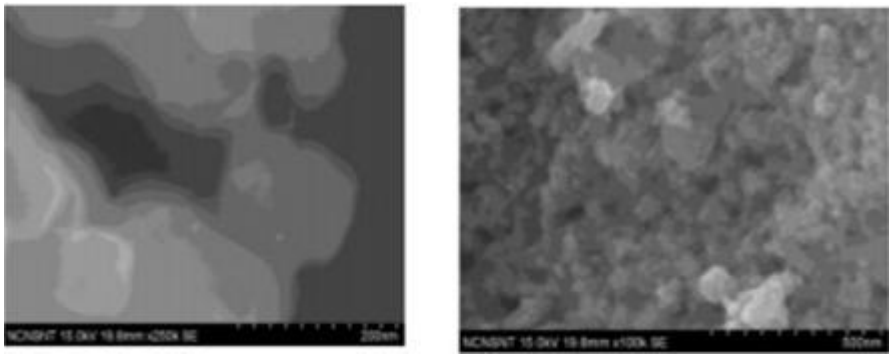

Figure 3.2: (a) FE - SEM images of WO_3. H_2O doped

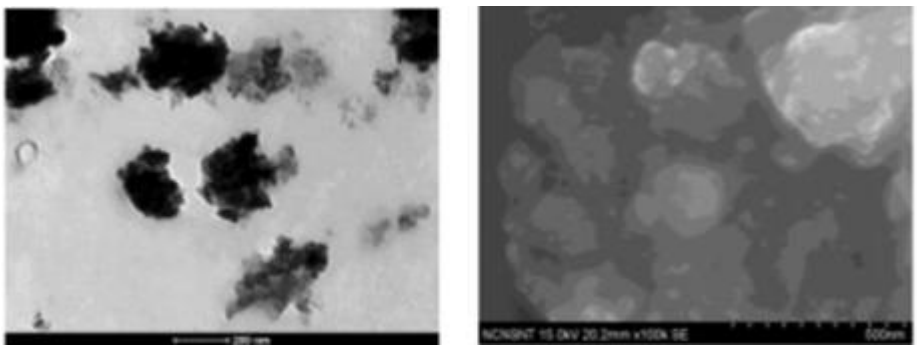

Figure 3.2: (b) FE - SEM images of annealed WO_3. doped

3.3 UV - VIS diffusion reflectance analysis (UV – VIS – DRS)

The UV VIS diffuse reflectance spectroscopy was carried out to know the optical properties of the pure and doped as prepared and annealed samples are shown in Fig.4.1. a) There are strong and wide reflectance peaks between the region 500 - 650 nm which indicated the prepared nanoparticles can display optical conductivity in the visible region. The maximum reflectance intensities have obvious blue shifts (as prepared samples) and redshifts (annealed samples) within the spectral region of 500 - 650 nm. The band gap energies for all the samples may be determined by using Kubelka - Munk (K - M model and its corresponding relation is given below. F (R) is the so - called remission or Kubelka – Munk function,

Where $R\infty = R\text{sample} / R\text{std}$

A graph is plotted between [F (R∞) hv] 2Vshvand the intercept value is the band gap energy Eg of the individual sample [20]. The band gap energies as a function of Magnesium concentration were found to be 3.27 and 3.33 eV respectively. On the contrary, in the case of annealed samples, the band gap energies in the identical doping conditions were 2.87 and 3.44 eV respectively. The reason for the increase in Eg (as prepared) may be explained using the Burstein - Moss (BM) [21] effect in which the lowest states in the conduction band are blocked and the allowed transitions can take place only to energies above Fermi level to unblocked valance level (between W6+ to Cu2+) due to the introduction of Cu2+ ion in the intermediate energy state. On the other hand, in the case of annealed samples, the increase in band gap energies as a function of dopant concentration is because exchange interaction between the band electrons of dx2 - y2 and day orbital of tungsten to the dx2 - y2 and dz2 orbital of Cu2+ ion. It gives rise to the positive correction in the valance band and leads to the narrowing of the band gap Fig.4.1 b).

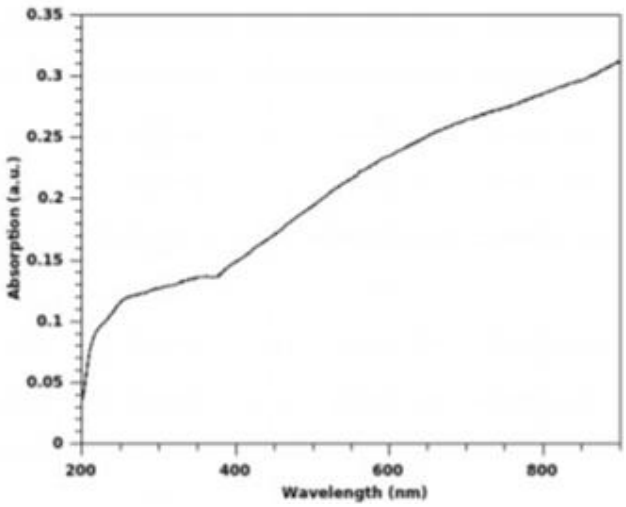

Figure 4.1: a) UV - VIS - DRS plots of doped WO_3. H_2O and WO_3

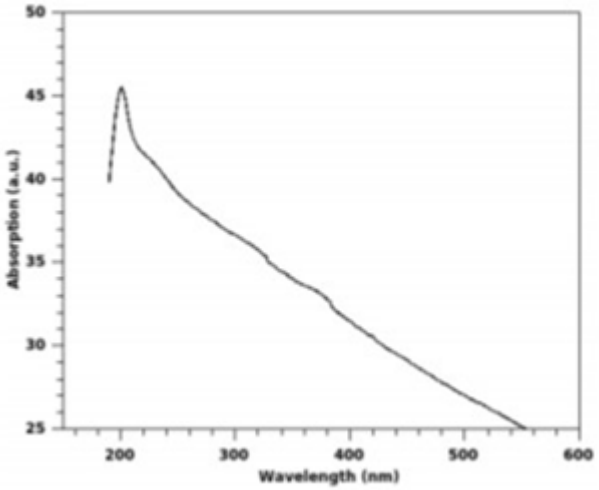

Figure 4.1: b) UV - VIS - DRS plots of doped WO_3. H_2O and WO_3

3.4 Magnetic behavior (VSM) Analysis

Fig.5.1 presents the hysteresis loops measured at room temperature of pure and copper doped respective tungsten oxide (WO3) nanoparticles. The measurements were performed on annealed samples since it has high crystalline nature with significant oxygen vacancies. It is to be understood that stoichiometric tungsten oxide may be exhibited dia magnetic behavior at room temperature and suits superconducting applications. Interestingly, The present prepared annealed both pure and doped exhibits the co - existence of both dia and ferromagnetic behavior [22] of the samples and may be attributed to the fact that the homogeneity in holes density due to the lack of oxygen (W17O47) which gives rise to the unpaired electrons in holes rich region enhanced the ferromagnetic behavior in addition with the dia magnetic nature. Subsequently, it can be seen from the Magnesium doped samples which are having light excess of oxygen than the pure sample could enhance the diamagnetic behavior at a negative magnetic field due to the stoichiometric oxygen content of the resultant annealed samples [23]. These unexpected results suggest that the doped samples try to persist well into the superconducting or diamagnetic state, namely the coexistence of dia and ferromagnetism in the hole - rich clusters. The enhancement of dia magnetic behavior in doped samples concerning the relative suppression of ferromagnetic behavior indicates the role of dopant in fixing the oxygen content and magnetic behavior of the end products, especially annealed samples.

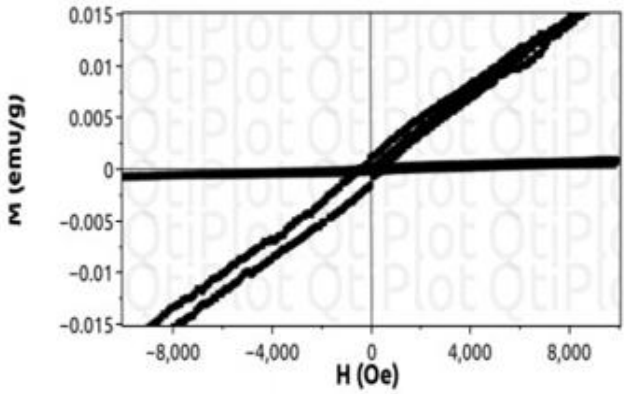

Figure 5.1: Room temperature hysteresis loops of WO_3 doped

Photo Catalytic Activity

Photocatalytic activity of annealed pure and “Cu” doped tungsten oxide (WO3) was investigated via the photo degradation of Rhodamine B dye under the illumination of UV light at room temperature. The sample of around 50 mg annealed samples as catalysts were dispersed in the ratio (2: 1) 80 mL / 4 mg. L - 1 Rhodamine B dye with an aqueous solution was taken in a 100 mL beaker and the suspension was stirred for 45 min to reach adsorption equilibrium in darkness condition. The suspension was further irradiated with 6W UV - lamp (Philips, Poland) at 254 nm during a continuous stirring process.7cm distance was maintained between the suspension and lamp. For every 30min the sample suspension was taken, centrifuged for 5 min and the concentration of rhodamine B in the suspension was found using UV - Vis (Ocean Optics, USA) spectrophotometer. The maximum absorption of rhodamine B was found to be 550nm [23]. The absorption spectra for tested compounds and their degradation rate are displayed in Fig.6.1. The linear degradation behavior of the sample clearly shows that

the dye is degrading under the visible region since the color of the rhodamine B is purple. The degradation efficiency of the tested compounds was calculated using the below formula,

$$Degradation\ efficiency\ \% = A0 - At\backslash A0\ x100$$

Where A0 and At are the absorbance at t = 0 and corresponding time respectively. The obtained degradation efficiency results imply "Cu" doped annealed WO3 sample is having highest degradation efficiency around 66.9% due to the formation of hydroxyl radical (OH°) and superoxide radical (O2°) at the band gap energy value of 2.87 eV. This result is in agreement with the UV - Vis diffused reflectance spectra analysis since it retains its stoichiometric oxygen content.

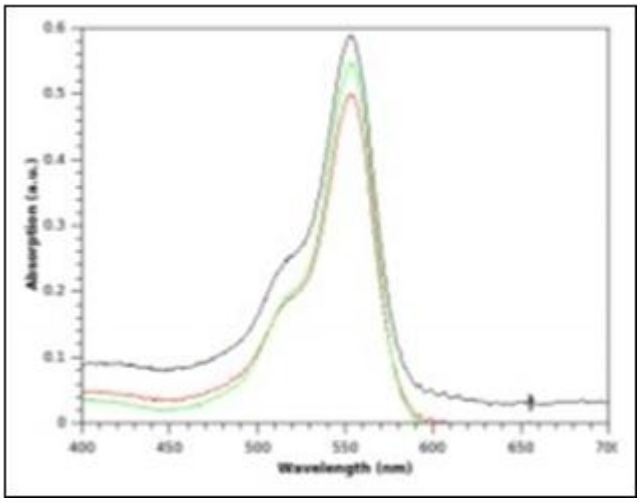

Figure 6.1 Room temperature photocatalyticanalysis on WO_3 doped

4. Conclusions

The present work focuses on the successful completion of pure and doped WO3. H2O by efficient microwave irradiation method in an ambient atmosphere. The successive crystalline phase of all the end products found that (Pure and Doped) with orthorhombic in phase. In the case of annealed samples, pure and doped samples (5wt. %) were found to become orthorhombic structures from Powder XRD analysis. Hence, these unexpected results suggested the role of dopants in fixing the oxygen content of the end product. UV - VIS - DRS studies will be evidence to know that the as - prepared samples have low optical conductivity than that of the annealed samples. This observation recommends the required optical conductivity can be attained by doping elements themselves instead of the annealing process. The interesting results from hysteresis loops suggested that the doped samples try to persist well into the superconducting or diamagnetic state than the pure sample suggesting that Cu - doped samples in association with the WO3 crystalline phase will be a promising candidate for superconducting and photocatalytic applications respectively.

References

[1] Tahir. M. B., Nabi. G., Rafique. M. Khalid. N. R, Nanostructuredbased WO3 photocatalysts: recent development, activity enhancement, perspectives and applications for wastewater treatment. Int. J. Environ. Sci. Technol. (2017), 14, 2519–2542.

[2] Salsa. V, Lemmer. Y, Malwela. T, Akande. A Beukes. M, Mwakikunga. B, Effect of varying ethanol and water compositions on the acetone sensing properties of WO3 for application in diabetes mellitus monitoring. Mater. Res. Express, (2020), 7, 035905.

[3] Hameed. A Gondal. M. A, Yamani. Z. H, Effect of transition metal doping on photocatalytic activity of WO3 for water splitting under laser illumination: role of 3d - orbitals. Catal. Commun. (2004), 5, 715 - 719.

[4] Baig. U, Gondal M. A., SuriyaRehman, Sultan Akhtar, Facile synthesis, characterization of nano - tungsten trioxide decorated with silver nanoparticles and their antibacterial activity against water - borne gram - negative pathogens. ApplNanosci2020, 10, 851–860.

[5] Duan. G, Chen. L, Jing. Z, Luna. P. D., Wen. L, Zhang. L, Zhao. L, Xu. J, Li. Z, Yang. Z, Zhou. R, Robust Antibacterial Activity of Tungsten Oxide (WO3 - X) Nanodots. Chem. Res. Toxicol.2019, 32 (7), 1357–1366.

[6] Matharu. R. K., Ciric. L, Ren. G, Edirisinghe. M, Comparative Study of the Antimicrobial Effects of Tungsten Nanoparticles and Tungsten NanocompositeFibres on Hospital Acquired Bacterial and Viral Pathogens. Nanomaterials 2020, 10, 1017, 1 – 16.

[7] Jeevitha. G, Abhinaya. R, Mangalaraj. D, Ponpandian. N, Tungsten oxidegraphene oxide (WO3 - GO) nanocomposite as an efficient photocatalyst, an antibacterial and anticancer agent. J PhysChem Solids 2018, 116, 137 - 147.

[8] Han. B, Popov. A. L, Shekunova. T. O, Kozlov. D. A, Ivanova. O. S, Rumyantsev. A. A, Shcherbakov. A. B, Popova. N. R, Baranchikov. A. E, Ivanov. V. K, Highly Crystalline WO3 Nanoparticles Are Nontoxic to Stem Cells and Cancer Cells. J. of Nanomaterials (2019).

[9] Ahamed. M, Hisham A. Alhadlaq, Majeed Khan. M. A, Karuppiah. P, Naif A. Al - Dhabi, Synthesis, Characterization, and Antimicrobial Activity of Copper Oxide Nanoparticles. J. of Nanomaterials (2014).

[10] Ghasempoura. F, Azimiradb. R, Aminic. AAkhavan. O, Visible light photoinactivation of bacteria by tungsten oxide nanostructures formed on a tungsten foil. Appl. Surf. Sci. (2015), 338, 55 - 60.

[11] Bankier. C, Matharu. R. K, Cheong. Y. K, Ren. G. G, Cloutman - Green. E, Ciric. L, Synergistic Antibacterial Effects of Metallic Nanoparticle Combinations. Sci. Rep. (2019).

[12] Syed. M. A, Manzoor. U, Shah. I, Habib Ali Bukhari. S, Antibacterial effects of Tungsten nanoparticles on the Escherichia coli strains isolated from catheterized urinary tract infection (UTI) cases and Staphylococcus aureus. New Microbiol, (2010), 33, 329 - 335.

[13] Ismail. R. A, Sulaiman. G. M, Abdulrahman. S. A, Marzoog. R. T, Antibacterial activity of magnetic iron

oxide nanoparticles synthesized by laser ablation in liquid. Mater. Sci. Eng. C. (2015), 53, 286 - 297.
[14] Turkez. H, Sonmez. E, Turkez. O, Mokhtar. Y. I, Stefano. A. D, Turgut. G, The Risk Evaluation of Tungsten Oxide Nanoparticles in Cultured Rat Liver Cells for Its Safe Applications in Nanotechnology. Braz Arch Biol, (2014), 57, 532 - 541.
[15] Popov. A. L, Savintseva. I. V, Popova. N. R, Shekunova. T. O, Ivanova. O. S, Shcherbakov. A. B, Kozlov. D. A, Ivanov. V. K., PVP stabilized tungsten oxide nanoparticles (WO3) nanoparticles cause hemolysis of human erythrocytes in a dose - dependent manner. Nanosystems: Physics, Chemistry, Mathematics, (2019), 10, 199 - 205.
[16] Akbaba. G. B, Turkez. H, Sonmez. E, Akbaba. U, Aydın. E, Tatar. ATurgut. G, Cerig. S, In vitro genotoxicity evaluation of tungsten (VI) oxide nanopowder using human lymphocytes. Biomed. Res. (2016), 27, 125 - 130.
[17] Chiu. Y. H, Mark. T. F, Chang, Chen. Y. C, Sone. M, Hsu. Y. J, Mechanistic Insights into Photodegradation of Organic Dyes Using Hetero structure Photocatalysts, Catalysts (2019).
[18] Palanisamy. G, Bhuvaneswari. K, Pazhanivel. T, Bharathi. G, Enriched, photocatalytic activity of Rhodamine B dye from aqueous solution using hollow sphere tungsten trioxide nanoparticles. Optik, (2020).
[19] Arshad. M, Ehtisham - ul - Haque. S, Bilal. M, Ahmad. N, Ahmad. AAbbas. M, Nisar. J, Khan. M. I, Nazir. A Ghaffar. AIqbal. M, Synthesis and characterization of Zn doped WO3 nanoparticles: Photocatalytic, antifungal and antibacterial activities evaluation. Mater. Res. Express, (2019).
[20] Hariharan. V, Parthibavarman. M, Sekar. C, Synthesis of tungsten oxide (W18O49) nanosheets utilizing EDTA salt by microwave irradiation method. J. of Alloy. And Comps. (2011), 509, 4788 - 4792, 2011.
[21] Hariharan. V, Radhakrishnan. S, Parthibavarman. M, Dhilipkumar. R, Sekar. C, Synthesis of polyethylene glycol (PEG) assisted tungsten oxide (WO3) nanoparticles for l - dopa bio - sensing applications. Talanta (2011), 85, 2166 - 2174.
[22] SarmientoArellano. J. S, Vega. A. K, Rosendo - Andrés. E, Díaz - Becerril. T, Romano - Trujillo. R, Oliva. A. I, De la Cruz. W, Lugo. J. M, Morales - Ruíz. C, Galeazzi - Isasmendi. R, García - Salgado. G, Nieto. F. G, Influence of HCl on the NPs - CdSe synthesis prepared by the colloidal method. J Appl Res Technol. (2016), 14, 225 - 231.
[23] Saleh. T. A, Principles, and Advantages of Microwave - Assisted Methods for the Synthesis of Nanomaterials for Water Purification. IGI Global Publisher of Timely Knowledge. (2017).